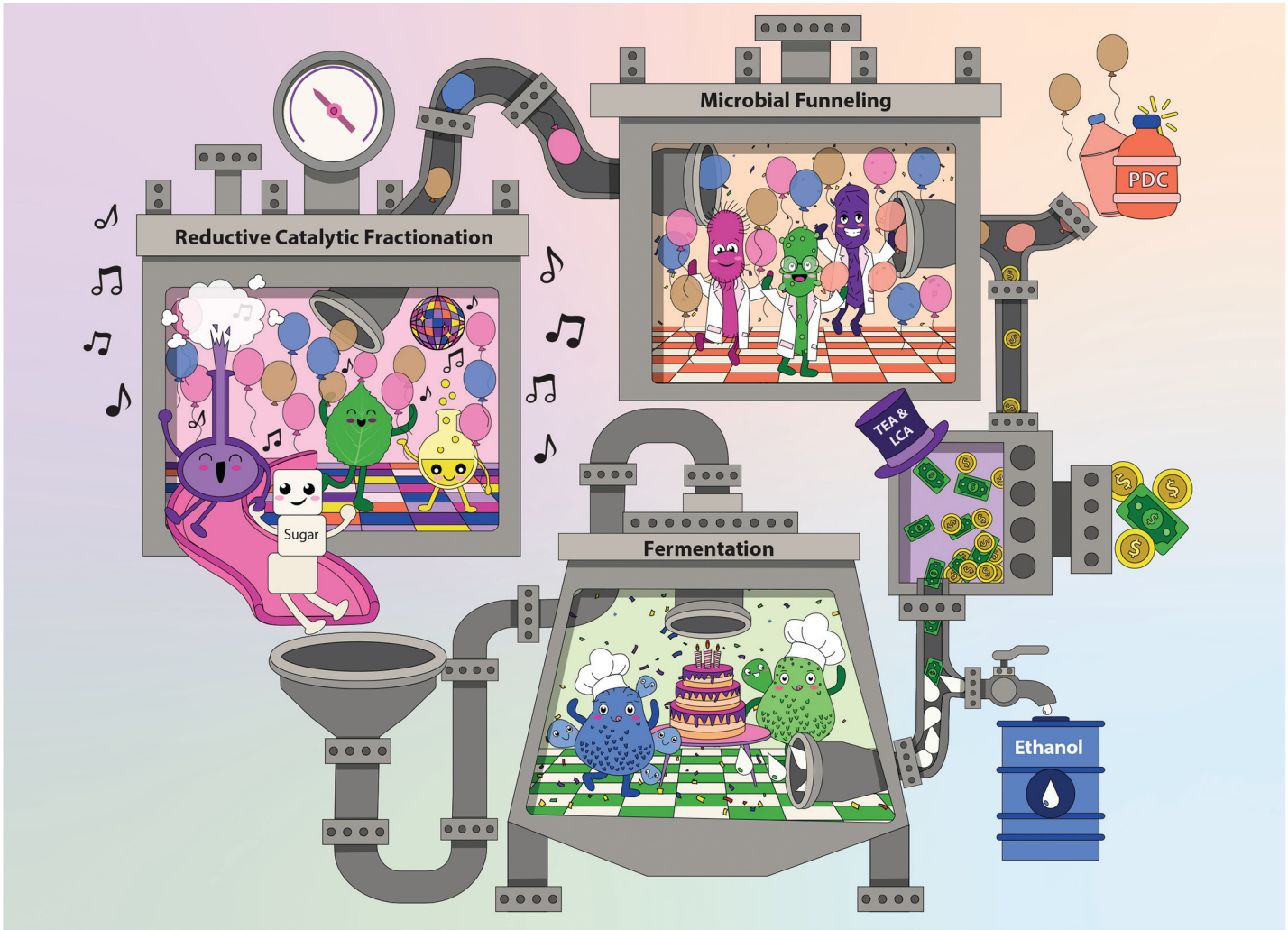

Showcasing research by Great Lakes Bioenergy Research Center research teams: Sener, Karlen, Donohue and Noguera *et al.* from the University of Wisconsin-Madison, and Maravelias *et al.* from Princeton University.

Integrating catalytic fractionation and microbial funneling to produce 2-pyrone-4,6-dicarboxylic acid and ethanol

A biomass-to-bioproduct processing chain was developed with the key step being reductive catalytic fractionation of the biomass into a lignin oil and pulp. The lignin oil was microbially funneled into 2-pyrone-4,6-dicarboxylic acid by an engineered microbe. The pulp was enzymatically digested, and the glucose and xylose were funneled to ethanol by an engineered yeast. Techno-economic and life cycle analyses of the RCF-based biomass-to-bioproduct processing chain were performed.

Image reproduced by permission of Canan Sener *et al.* from *Green Chem.*, 2026, **28**, 186.

Cover artwork created by Chelsea Mamott from Wisconsin Energy Institute, https://www.linkedin.com/in/chelseamamott/

As featured in:

See Canan Sener *et al.*, *Green Chem.*, 2026, **28**, 186.

ROYAL SOCIETY OF CHEMISTRY

rsc.li/greenchem

Registered charity number: 207890

Green Chemistry

PAPER

View Article Online
View Journal | View Issue

Cite this: *Green Chem.*, 2026, **28**, 186

Integrating catalytic fractionation and microbial funneling to produce 2-pyrone-4,6-dicarboxylic acid and ethanol

Canan Sener, *†[a,b] Emmanuel A. Aboagye, †[c] Steven D. Karlen, [a,b] Jose M. Perez, [a,b,d] German E. Umana,[a,b,d] Yaoping Zhang,‡[a,b] José Serate,[a,b] Timothy J. Donohue, [a,b,e] Daniel R. Noguera [a,b,d] and Christos T. Maravelias [c,f]

Replacing biorefinery designs that use stepwise fractionation, depolymerization, and conversion processes with designed tandem process steps can greatly reduce a biorefinery's operating costs and environmental impact. Reductive Catalytic Fractionation (RCF) is a highly efficient lignin-first approach that combines biomass fractionation and lignin depolymerization to generate a hydrogenolysis oil and pulp. The oil is composed of a complex mixture of phenolic monomers, dimers, and oligomers. Intergrating this chemical deconstruction process with microbial funneling of phenolics can simplify the product mixture and make high-value products. We applied RCF to poplar biomass in a biomass-to-bioproduct processing chain in which the phenolics were funneled to 2-pyrone-4,6-dicarboxylic acid (PDC) by an engineered strain of *Novosphingobium aromaticivorans* DSM12444. The pulp was enzymatically digested and the glucose and xylose was funneled to ethanol by an engineered strain of *Saccharomyces cerevisiae* GLBRCY945. By combining biomass fractionation and lignin depolymerization we removed a costly processing step that directly translated into a 29% reduction in the minimum selling price of PDC. This work combines experimentation with process modeling of an integrated biorefinery design to show how utilizing tandem process steps can significantly reduce operating expenses and environmental impact of upgrading lignocellulosic biomass to a portfolio of high value products.

Received 1st August 2025,
Accepted 15th October 2025

DOI: 10.1039/d5gc03986j

rsc.li/greenchem

Green foundation

1. In this study, we compare the economic and environmental impact of two biorefinery designs to convert poplar biomass to PDC, a bioplastic precursor, and ethanol, a biofuel that could be converted to sustainable aviation fuel (SAF).
2. The TEA and carbon footprint analysis of the two biorefinery designs shows that the impact of converting biomass to PDC and ethanol could be improved by combining biomass fractionation and lignin depolymerization into a single process step.
3. This study used methanol as the processing solvent, future studies that explore greener solvents and solvent mixtures could further reduce the carbon footprint and environmental impact of the biorefinery.

Introduction

When designing viable biorefineries, it is imperative to maximize the value obtained from all components of lignocellulosic biomass. As a bountiful source of renewable carbon for the sustainable production of fuels and chemicals, the polysaccharide fraction (70–85 wt% of the dry weight) has been extensively studied and various processes have been developed to produce valuable liquid fuels and commodity chemicals. The lignin fraction (15–30% of the dry weight) is often burned to generate process heat and electricity, as it has traditionally been difficult to fractionate and isolate lignin in a condition that is amenable to downstream utilization. The

[a]*Great Lakes Bioenergy Research Center, University of Wisconsin-Madison, Madison, WI, USA. E-mail: csener@wisc.edu*
[b]*Wisconsin Energy Institute, University of Wisconsin-Madison, Madison, WI, USA*
[c]*Department of Chemical and Biological Engineering, Princeton University, Princeton, NJ, USA*
[d]*Department of Civil and Environmental Engineering, University of Wisconsin-Madison, Madison, WI, USA*
[e]*Department of Bacteriology, University of Wisconsin-Madison, Madison, WI, USA*
[f]*Andlinger Center for Energy and the Environment, Princeton University, Princeton, NJ, USA*
†These authors equally contributed to this work.
‡Dr Zhang passed away before the submission.

efficiencies of a modern pulp mill's heat and energy integration has resulted in an excess of lignin, as burning all the lignin results in ~200% of the requirements. Their remote location makes utilization of surplus heat and energy outside of the pulp mill challenging. As lignin is the largest source of renewable aromatics and is produced in excess, researchers are exploring economically viable strategies to convert half of the lignin into drop-in bioderived alternatives to currently fossil-derived compounds.

"Lignin-first" biorefineries could be designed to maximize the conversion of the entire lignocellulosic biomass into fuels and chemicals in a manner that is not solely focused on the polysaccharides.[1,2] Many of these strategies use solvolysis to liberate the lignin from the plant cell walls in a "native-like" form, with or without protecting-groups,[3] then depolymerize the lignin through catalytic processing.[4–7] This approach is performed using one of two biorefinery designs (Fig. 1):[8] (1) using discrete stepwise processes of biomass fractionation (lignin solvolysis), lignin depolymerization (*e.g.*, hydrogenolysis), and monomer up-conversion to fuels and chemicals; (2) starting with a concerted processes in which lignin solvolysis and depolymerization occur within the same "pot", although typically still following a stepwise mechanism, followed by monomer up-conversion to the target fuels and chemicals.

Hydrogenolysis is an efficient method of depolymerizing lignin into a mixture of phenolic monomers, dimers, and oligomers (Fig. 1C). The chemical composition of the mixture is dependent on the processing conditions, *e.g.*, catalyst, reaction temperature, reaction time, and lignin feedstock. When hydrogenolysis and lignin fractionation steps are combined, it is sometimes referred to as "Reductive Catalytic Fractionation" (RCF).[9–11] The RCF process produces a similar phenolic mixture (lignin oil) dissolved in the reaction solvent, and a low-lignin pulp (polysaccharide-based solid residue). These two product streams can be further refined into discrete target products.

In previous work,[12] we evaluated a discrete stepwise (type 1) lignin-to-bioproduct processing chain that combined chemical and biological upgrading in tandem to extract greater value from the lignin fraction (Fig. 1A). This processing chain started with isolation of lignin from lignocellulosic biomass under mild organosolv fractionation conditions using γ-valerolactone (GVL) and water as the solvent system with dilute sulfuric acid as a catalyst.[9] In this scheme, lignin degradation was minimized during the biomass fractionation by the short residence time and low process temperatures (<120 °C).[13] Lignin depolymerization by hydrogenolysis in methanol with Pd/C as catalyst, was followed by hydrogen and methanol recovery to generate a lignin oil, that was fractionated into phenolic monomers and phenolic oligomer streams. The oligomer stream was used to generate process heat and electricity. Through microbial funneling, the resulting phenolic monomers were converted to 2-pyrone-4,6-dicarboxylic acid (PDC), a surrogate target compound for a microbially produced value-added product and a gateway into microbial central metabolism.[12] PDC isolation was modeled by

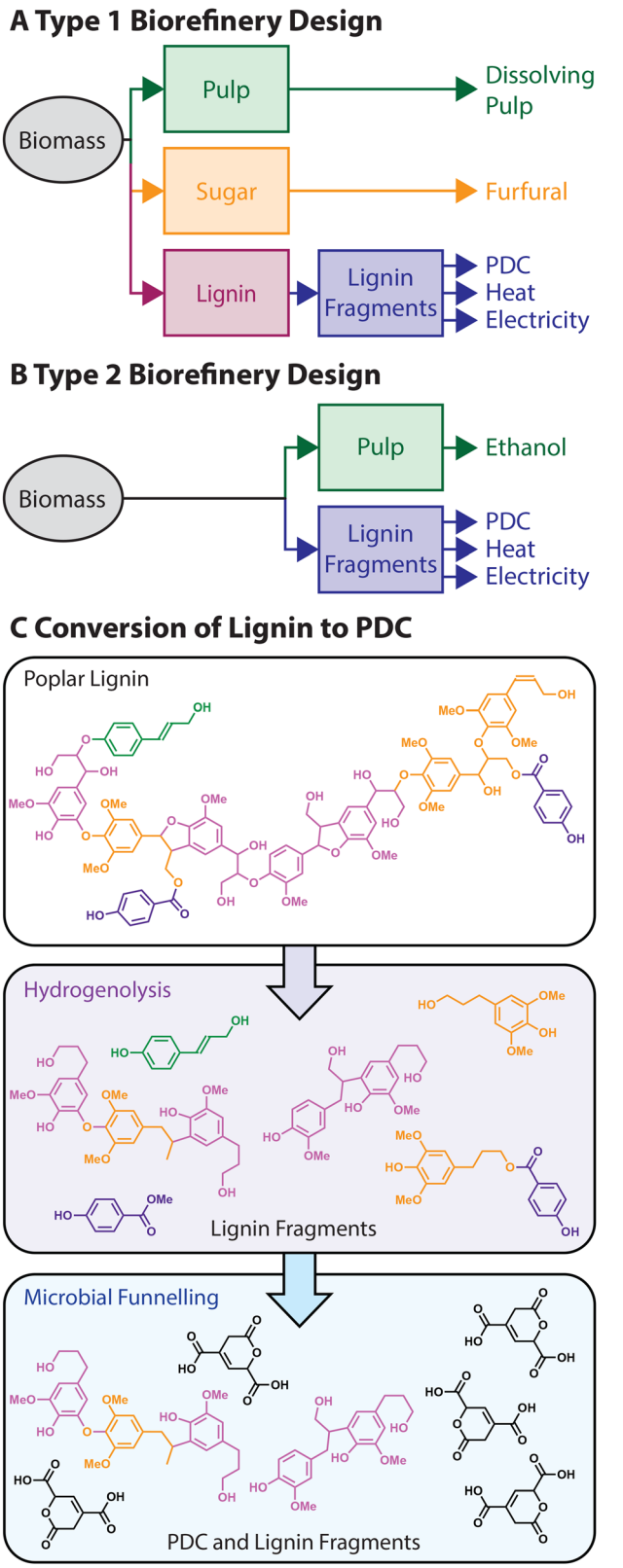

Fig. 1 Schematical representation of lignin-first approaches to lignocellulosic biomass valorization. (A) Type 1, utilizing highly controlled discrete stepwise processing stages. (B) Type 2, capitalizes on value-added benefits of concerted synergistic process stages. (C) Visualization of hydrogenolysis based lignin depolymerization integrated with microbial funneling of phenolic monomers to PDC.

crystallization as the sodium salt $Na(PDC)_2$. A minimum selling price (MSP) for $Na(PDC)_2$ salt was initially estimated at \$12.10 per kg (2019\$, which is equivalent to \$15.9 per kg in 2024\$) using conventional hydrogenolysis reactors and it increased to \$19.70 per kg (2019\$, which is equivalent to \$25.9 per kg in 2024\$) when thicker reactor walls were considered to account for the pressure during hydrogenolysis. The techno-economic analysis (TEA) of this process focused solely on lignin valorization, adjusting the cost of lignin based on the production of dissolving pulp and furfural from the polysaccharides as was previously modeled for the GVL biorefinery (Fig. 1A),[9] resulting in two new products (PDC salt and electricity) being reported.

Building on this prior work, the present study considers an integrated lignin-first biorefinery design (type 2) that replaces the steps of GVL fractionation and lignin hydrogenolysis with a single RCF step,[14] and considers how the lignin and carbohydrate fractions would be utilized. Using RCF increases the monomer/oligomer product yield on a per kg of biomass basis through two synergistic effects; (1) by retaining the soluble metabolites (*e.g.*, glycosylated *p*-hydroxybenzoate)[15] and small lignin fragments that were lost in the lignin isolation stage of the GVL-fractionation process; and (2) by increasing the fraction of lignin in the biomass that is depolymerized to the RCF oil through elimination of acid catalyzed lignin decomposition and condensation. We show that, using an engineered strain of *Novosphingobium aromaticivorans* DSM12444, the complex mixture of aromatic compounds produced by RCF can be upgraded to PDC,[12] while the low-lignin carbohydrate pulp was enzymatically hydrolyzed and fermented to ethanol without any observed inhibitory issues. Switching to an RCF based (concerted) lignin-first biomass-to-bioproduct processing chain removed the most expensive stage of the previous (discrete stepwise) lignin-to-bioproduct (PDC) processing chain and resulted in a \$7.5 per kg (29%) reduction in the MSP of PDC.

Results and discussion

Untreated biomass *vs.* high quality lignin from the GVL-biorefinery

High-quality lignins are close in chemical structural composition to native lignin, meaning that β-O-4 linkages are >50% of the inter-unit linkages and the C–C bonds are limited to those formed through radical coupling during lignification (β–β, β–5, and 5–5) and not through condensation of partially depolymerized lignins. In this discussion we exclude derivatized (protected) lignin structures that, by their nature, are not native and require special consideration in downstream processing. The lignin extraction conditions determine the degree of lignin depolymerization and condensation. As a result, there have been several different proposed GVL-biorefinery designs.[9,16] One aspect that differentiates them is whether they produce a high-quality lignin stream. The initial design involved a single high temperature process that dissolved all of the biomass, but at the expense of forming a heavily condensed lignin.[16] On the other end of the spectrum the design uses a lower process temperature to extract a high-quality lignin to produce carbon foam as part of a product portfolio containing dissolving pulp, and furfural.[9]

In our previous study,[12] we explored a lignin-to-bioproduct processing chain designed to increase the value of the high-quality lignin, isolated from the GVL-biorefinery (Fig. 1A), to PDC (a surrogate for microbially derived commodity chemical products).[12] We linked hydrogenolysis of the lignin with microbial funneling to produce PDC from a variety of biomass feedstocks (poplar, maple, switchgrass, and sorghum). Technoeconomic analysis identified the major bottlenecks of this lignin-to-bioproduct processing chain. The analysis showed the lignin : solvent (methanol) ratio in the hydrogenolysis greatly impacted the MSP due to the need to recover and recycle >99% of the solvent. As most of the PDC was produced from only the phenolic monomers (Ar_{PrOH}, Ar_{Me}, arylesters, and arylcarboxylic acids), distillation of those components from the oligomers would enable the use of the oligomers for process heat and energy. Accounting for these constraints, the TEA indicated that the lignin was nearly 40% of the cost of the entire lignin-to-PDC processing chain.

Looking more closely at the whole GVL-biorefinery identifies several drawbacks to the stepwise biorefinery design illustrated in Fig. 1A. (1) The yield of isolated high-quality lignin (77% β-O-4) is ~22% of the total lignin, 5.3 wt% of the biomass, Table 1. (2) Lignin precipitation and subsequent GVL recovery is costly and energetically expensive. (3) The acidic organosolv process partially depolymerizes the lignin reducing the β-O-4 content by 9% and generating a more condensed lignin that is enriched in C–C linkages. (4) Some of the shorter lignin chains, phenolic monomers, phenolic acids, and soluble metabolites are lost in the lignin isolation step. These and other aspects of the GVL-biorefinery design made us question the use of lignin isolated in the stepwise approach (Fig. 1A) and instead to use RCF, a design that combines biomass fractionation and hydrogenolysis into one process (Fig. 1B). In RCF the lignin is extracted from the biomass in the presence of a catalyst, either dispersed in the sample, contained within catalyst cages, or placed in-line with the eluting solvent stream. The goal is to introduce the catalyst that is needed to depolymerize the lignin to chemically stable products before significant amount of lignin condensation can occur. The advantage of a catalyst cage and in-line catalysis is in separation of the catalyst from the delignified biomass; however, the disadvantage is that the lignin spends more time in solution before it can get to the catalyst and therefore has a higher degree of unfavourable condensation events. Using a dispersed catalyst reduces the mass transport issues but requires downstream separation and recovery of the catalyst from the delignified biomass. To allow comparison with the previous study, we selected to use a dispersed micron-sized Pd/C catalyst which could be separated by filtration from the hydrolysate produced by enzymatic digestion of the pulp. The filtered sugar stream did not contain unexpected inhibitors

Table 1 HSQC NMR characterization and hydrogenolysis product distribution obtained from lignin isolated from low-temperature GVL-extraction and whole-cell-wall poplar

NMR analysis[b]	Isolated lignin[a]	Biomass
$S:G$	68 : 32	63 : 37
S/G	2.15	1.72
$(S^{\star}/S)^{c}$	0.35	0.06
Cinnamaldehyde end-groups	3%	3%
*p*HBA	26%	20%
β-O-4 : β–5 : β–β[d]	77 : 15 : 8	86 : 7 : 7
Phenolic monomer composition	**Lignin hydrogenolysis**	**RCF**
$S:G$	63 : 37	62 : 38
S/G	1.69	1.65
S_{PrOH}	35.8%	45.8%
G_{PrOH}	26.0%	30.2%
H_{PrOH}	1.3%	4.2%
S_{Pr}	14.0%	7.2%
G_{Pr}	1.4%	0.8%
H_{Pr}	3.7%	0.0%
Me-*p*HB	11.0%	8.7%
Truncated sidechain	6.6%	3.1%
Phenolic monomers wt% of biomass	1.1% (19.9% lignin)	11.0%
Isolated lignin wt% biomass	5.3%	N/A

[a] Perez *et al.* 2022.[12] [b] Values reported on a $[0.5 \times (S_{2/6} + S'_{2/6}) + (G_2) = 100]$ basis; as a terminal units and pendent groups these components are overrepresented in the NMR data. [c] The condensed *S*-units (*S*⋆) correlation signal increases in abundance *vs.* the *S*-units ($S_{2/6}$ + $S'_{2/6}$) correlation signals as the lignin gets more condensed. [d] Values reported on a $[A_a + B_a + 0.5 \times (C_a + C'_a) = 100]$ basis. N/A = not applicable.

from the process. The hydrogenolysis conditions were only slightly modified from our previous study to account for the use of raw biomass in place of the isolated lignin that is soluble in methanol at hydrogenolysis temperatures. We chose to continue with methanol as a low boiling point solvent so that we could directly compare the results of this tandem biomass-to-bioproduct process with the prior lignin-to-bioproduct chain.

Hydrogenolysis of poplar

The hydrogenolysis oil formed under the hydrogenolytic reaction conditions used, was analyzed *via* GC/FID. As expected from previous studies,[17,18] the aromatic monomer product distribution from the isolated lignin and raw biomass (not pretreated), with Pd/C as the catalyst, heavily favored the production of arylpropanol (Ar_{PrOH}) over arylpropane (Ar_{Pr}) or components with truncated [arylethyl or arylmethyl] sidechains, as shown in Table 1; the Ar_{PrOH} : Ar_{Pr} ratio from the isolated lignin was 77 : 23, whereas it was 91 : 9 from poplar biomass. The increase of 14% Ar_{PrOH} from the biomass correlates with a decrease of 2.3% Me-*p*HB. When the γ-hydroxy of a β-aryl ether is acylated, the hydrogenolytic depolymerization pathway can proceed *via* the γ-acylated monolignol (*e.g.*, sinapyl *p*-hydroxybenzoate), from which palladium assisted elimination of the allylic ester forms the free *p*-hydroxybenzoic acid and a terminal 3-(aryl)propene.[19] Subsequent hydrogenation leads to Ar_{Pr}.[19] The increase in relative Ar_{PrOH} content from biomass is favorable in the microbial funneling of hydrogenolysis products to PDC. As we showed in previous work, an engineered *N. aromaticivorans* strain can convert Ar_{PrOH}, Ar_{Me}, arylpropionate, and hydroxy-benzoates to PDC.[12] The Ar_{Pr} and Ar_{Et} species are oxidized on the α-carbon to a mixture of α-alcohols and α-ketones. Overall, the fraction of aromatic monomers expected to be funneled to PDC by the engineered *N. aromaticivorans* strain was 78% for the isolated lignin and 92% from biomass.

Biological conversion

There are many potential bioreactor designs for funneling these solutions of phenolic compounds into the target PDC product, all of which have pros and cons that are application dependent. For example, running in batch mode with a single feed (fill, inoculate, incubate), subjects the microbe to the highest possible inhibitions from substrate toxicity. However, if the same volume of feed media is added to the batch reactor in a series of smaller additions, the microbes have a chance to detoxify the solution (*e.g.*, conversion to PDC) and keep the substrate concentration below toxicity. This was demonstrated for *N. aromaticivorans* strain PDC using a continuous membrane flow reactor design, achieved steady state PDC concentrations over 50 mM, with no inhibition.[20]

N. aromaticivorans strain PDC converts a wide array of lignin derived phenolics to PDC. This variety of validated substrates consistently increases and includes the major hydrogenolysis products,[12] oxidation products (*e.g.*, aromatic ketones, aldehydes, and acids),[21] aromatic amides,[22] and the β-O-5 dimer, which converts into two PDC units.[23]

For this study, we used a simple proof of validity assay to determine the yield of PDC from phenolic compounds in the hydrogenolysis oil that could achieved if the substrates in the

feed solution are kept below the threshold of toxicity. Our approach diluted the hydrogenolysis oil in a minimal growth media (see Experimental section) that was supplemented with glucose to provide a carbon source for bacterial growth.[12,21,22] This dilution reduced the methanol concentration to below the toxicity and growth inhibition threshold for *N. aromaticivorans* and ensured that we were able to accurately measure the amount of hydrogenolysis oil phenolics added to each culture. The dilute hydrogenolysis oil medium was mixed with a fresh culture of the PDC-producing strain of *N. aromaticivorans* at a ratio of 1 : 1 v/v to allow growth and avoid the lag phase. An abiotic control was prepared by mixing the same glucose-supplemented medium containing diluted hydrogenolysis oil with sterile medium at a ratio of 1 : 1 v/v. Microbial growth and the concentration of phenolic monomers and PDC in the different cultures and the abiotic control was monitored periodically during the experiments (Fig. S1).

PDC accumulation in the culture medium from isolated lignin hydrogenolysis oil reached a maximum concentration of 0.19 ± 0.01 mM, which converted to a calculated yield of 139.1 ± 0.3 g PDC kg^{-1} lignin, Table 2.[12] When the combination of lignin isolation, hydrogenolysis, and microbial conversion product yields were included into the yield determination the maximal concentration represented 7.52 ± 0.02 g PDC kg^{-1} poplar.[12] In this scenario, the GVL-biomass fractionation coupled to a lignin-to-bioproduct processing chain, the portfolio of products include: PDC, dissolving pulp, furfural, and electricity (generated from the condensed lignins).

PDC accumulation in the culture medium from RCF oil produced from raw biomass reached a maximal concentration of 0.15 ± 0.01 mM, which converts to a calculated yield of 58.5 ± 3.5 g PDC kg^{-1} poplar, Tables 2 and S1. The product portfolio from this scenario #2 consists of: PDC, ethanol, and electricity.

Comparing the two scenarios, the yield of PDC from raw biomass increased by 7.8-fold *vs.* the isolated lignin. We propose that the increase in PDC yield comes from: (1) higher efficiency lignin depolymerization to phenolic monomers during RCF as compared to hydrogenolysis of GVL-extracted lignin, in which most of the lignin remained with the biomass or was condensed; (2) higher arylpropanol content in the RCF oil also increased the potential maximal yield of PDC; and (3) retention of phenolic monomers and soluble lignin fragments in the RCF oil that are typically lost during lignin isolation using GVL or other approaches.

Enzymatic digestion

Limiting the amount of lignin condensation requires minimizing the amount of time that the polymer is in solution without being stabilized through catalytic reduction (or other mechanisms). In this work, we use RCF to generate monomeric phenolics as depolymerization products. The maximal yield of such a process occurs when the catalyst is dispersed in the biomass, however this results in a hydrogenolysis pulp containing the catalyst. In RCF, the polysaccharide fraction is destined for enzymatic saccharification and microbial conversion. To determine if the presence of the heterogenous catalyst or hydrogenolysis formed compounds that had a negative impact on polysaccharide saccharification, we treated the RCF pulp with cellulase enzymes to generate a hydrolysate containing 100 g L^{-1} glucose and 42 g L^{-1} xylose, Table S2. At this point, the Pd/C catalyst was recovered from the hydrolysate *via* filtration. The hydrolysate was then inoculated with yeast strain Y945 to monitor growth and ethanol production (Fig. S2A). The ethanol production yield of 85.3%, Table 2, and yeast growth rates did not indicate the presence of inhibitors derived from the heterogenous catalyst or hydrogenolysis residue in the RCF pulp. Comparison of the growth curves with and without the addition of yeast extract supplement indicated a slight deficiency in nutrients in the hydrolysate, but no significant reduction in ethanol yield (Fig. S2B).

Process synthesis

Based on the obtained experimental data, we modelled an integrated biomass-to-PDC process using RCF for biomass fractionation and lignin depolymerization (Fig. 2). A general block flow diagram of the biorefinery which consists of nine major blocks: (1) reductive catalytic fractionation of biomass (RCF), (2) monomer purification (MNP), (3) PDC production (PDCP), (4) isolation of PDC product (PDCI), (5) hydrolysis of carbohydrate-pulp (HYD), (6) fermentation of sugars to ethanol (FERM), (7) ethanol separation and recovery (SEP), (8)

Table 2 HPLC-quantified values for the microbial conversion experiments

Phenolic monomer to PDC	Isolated lignin[a]	Biomass
Maximal [PDC] (mM)	0.19 ± 0.01	0.15 ± 0.01
g PDC kg^{-1} lignin	139.1 ± 0.3	N/A
g PDC kg^{-1} poplar	7.52 ± 0.02	58.5 ± 3.5
Composition of hydrolysate produced from RCF pulp	**Before fermentation**	**After fermentation**
Glucose (g L^{-1})	101.5	0
Xylose (g L^{-1})	43.1	16.4
Cellobiose (g L^{-1})	6.3	2.1
Ethanol (g L^{-1})	0	52.6
Ethanol yield	N/A	85.3%

[a] Perez *et al.* 2022.[12]

wastewater treatment (WWT), and (9) combined heat and power generation (CHP).

In this process model, biomass, methanol, and hydrogen (streams 1, 2, and 3) are introduced into RCF reactors in the presence of a 5 wt% Pd/C catalyst in the RCF block for a residence time of 2 hours; see Table S3 in SI for biomass composition. After reaction, the methanol and hydrogen are recovered and recycled to minimize fresh solvent and reductant requirements; see Fig. S3 in SI for details. The monomer, oligomer, and carbohydrate pulp stream is sent for solid–liquid separation through which the polysaccharides are separated from the lignin-derived fraction. The recovered carbohydrate-pulp (stream 4) is routed to the HYD and FERM blocks for enzymatic hydrolysis and fermentation to ethanol, respectively, with ethanol recovered (stream 11) in the SEP block, following a process consistent with that used by Humbird *et al.*[24]

Stream 6 containing phenolic monomers, oligomers, and residual methanol is directed to the MNP block where a distillation column with a partial condenser is used for monomer recovery (Fig. S3). Residual methanol is removed in the column overhead vapor stream for recycling back to the RCF block (stream 14). The distillate stream, rich in monomer (stream 15), is directed to the PDCP block where the monomers are biologically converted into PDC *via* microbial funneling, while the oligomers (stream 16) are sent for heat and power generation.

Stream 17 is the growth media needed to support microbial funneling of the biomass derived phenolics to PDC. The resulting extracellular media containing PDC (stream 18) is sent to the PDCI block, in which PDC is precipitated as a sodium salt isolated using sodium chloride (stream 19), and recovered as final product (stream 21), while the process wastewater (stream 20) is sent for wastewater treatment. Catalyst separation was modeled under the assumption of negligible loss or breakthrough, consistent with steady-state operation in an *n*-th plant design. The process model for RCF and MNP blocks were developed and simulated using ASPEN PLUS (V14), with the corresponding detailed process description and operating conditions provided in Fig. S3.

Techno-economic analysis (TEA)

A TEA of this process calculated a MSP for $Na(PDC)_2$ salt of \$18.39 per kg (Fig. 3A). The largest cost contributor is the RCF block, accounting for 67.0% of the MSP. Within the RCF block, the capital cost of reactors and solvent recovery equipment are the primary drivers, contributing \$8.19 per kg. Material costs in the RCF block also play a significant role, with feedstock costs contributing \$1.95 per kg, with the remainder primarily deriving from makeup methanol. Other substantial costs are incurred in the heat and power generation block, with capital costs contributing 10.6% to the MSP. However, these costs are partially offset by \$0.14 per kg from excess electricity (8 MW) sold to the grid. The PDCP block contributes 11.4% of the production cost to the MSP, primarily driven by the cost of growth media for biological funneling, which accounts for 7.6%, see Table S4 in SI for detailed capital and operating costs.

Due to the substantial amount of solvent required to achieve effective biomass fractionation and lignin depolymerization, heat integration in the RCF block is crucial for minimizing the overall heat duty of the biorefinery. To achieve this, we implemented two main techniques. Firstly, the reactor's effluent stream was processed through a series of flash separation steps allowing for a gradual reduction in solvent content (Fig. S3). As a result, the energy requirements of subsequent equipment – particularly the distillation columns – are minimized, improving the overall energy efficiency of the biorefinery. Secondly, we employed heat exchangers to recover heat from the vapor streams from the flash units to preheat the recycled solvent, reducing the heating required to bring the recycled stream to reactor conditions. These two improvements lead to ~78% heat load reduction. The analysis was conducted under the "*n*th-plant" assumption, implying that the system operates under steady-state conditions. As such, the heat-integration scheme is evaluated based on steady-state operation rather than short-term dynamic disturbances.

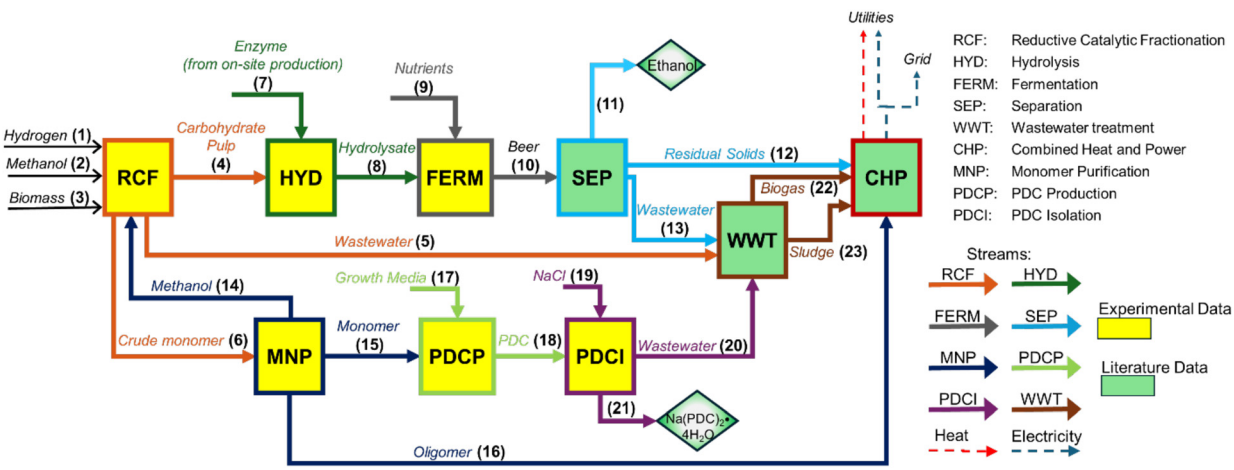

Fig. 2 Block flow diagram of the biorefinery. Stream numbers are in parentheses.

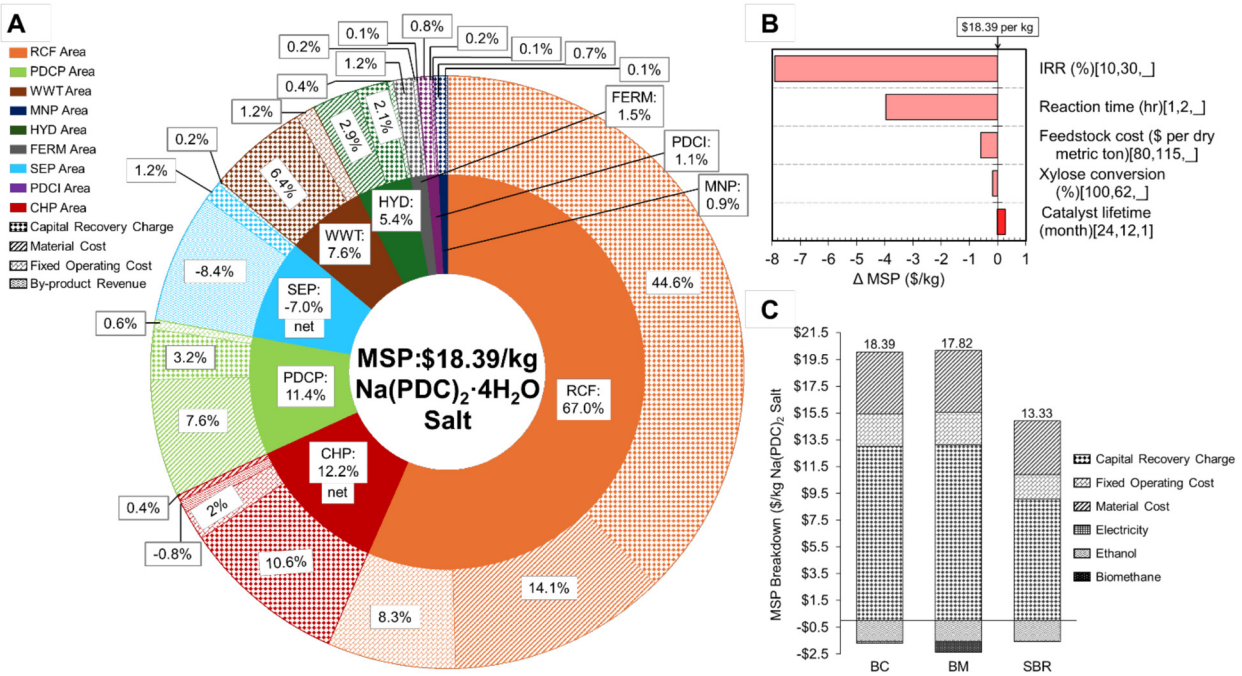

Fig. 3 (A) Cost distribution for MSP of PDC salt. Cost contributions of blocks given in the inner circle, while capital, material, and fixed operating costs are given in the outer circle. The cost of on-site enzymatic production is included in the HYD block (B) sensitivity analysis (C) $Na(PDC)_2$ salt MSP for two alternative cases. Abbreviations: BC: Base case; BM: Biomethane case; SBR: Solvent-to-Biomass Ratio case.

We also conducted a single-point sensitivity analysis to identify important process and economic parameters (Fig. 3B). Reducing IRR from 30% (we use a higher IRR due to higher investment risks associated with new technology) to 10% as in NREL reports results in the highest reduction (~43%, $7.91 per kg) in the MSP; due primarily to the changes in the discounting factors. Similarly, decreasing the RCF reaction time from 2 to 1 hour leads to a ~22% reduction ($3.97 per kg) in the MSP. Reduction in catalyst lifetime from 1 year to 1 month increases the MSP by $0.27 per kg, while longer lifetime of 2 years reduces the MSP by $0.01 per kg. Reduction in biomass feedstock cost and increase in xylose-to-ethanol conversion have the least impacts (3%, and 1%, respectively) on the MSP.

The TEA is extended to assess two cases: (1) selling biomethane as a co-product rather than converting it to excess electricity, and (2) reducing the solvent-to-biomass ratio from 17.25 : 1 to 12 : 1 (Fig. 3C). Selling biomethane reduces the MSP by 3%, mainly due to both capital savings and additional revenue credits associated with selling biomethane as a renewable fuel. From a capital cost perspective, producing excess electricity using a turbogenerator requires a higher investment compared to upgrading biogas to biomethane using a pressure swing adsorption, which also benefits from an investment tax credit (ITC).[25] On the revenue side, selling biomethane as a co-product results in revenue streams from renewable identification number (RINs) under the renewable fuel standard program,[26] and clean fuels production credit (CFPC).[27] Reducing the solvent ratio has the highest impact on MSP (~28% reduction) because lower solvent usage decreases RCF reactor size and associated capital costs and reduces capital expenses and heating demands for solvent recovery.

Fig. 4 shows the mass and energy flows in the biorefinery normalized to 1 kg of $Na(PDC)_2$ salt production. We observe that about 22.27 kWh (~85%) of total heat is used for solvent recovery and monomer purification in the RCF and MNP blocks, while ~50% (4.26 kWh) of electricity is used in the RCF block, mainly for hydrogen compression.

Carbon footprint analysis

The net carbon footprint of the process is 0.98 kg CO_2e per kg of $Na(PDC)_2$ salt (Fig. 5A). The delivered feedstock has the highest impact with biomass soil organic carbon sequestration contributing a credit of −2.12 kg CO_2e per kg. Offsetting emissions from gasoline based on the produced ethanol contributes significantly to the carbon credits, whereas the electricity offset, based on the average U.S. electricity grid, also provides substantial reduction of −0.64 kgCO_2e per kg of product.

There is a higher contribution from the RCF block due to make-up solvents and catalyst losses (~5% losses assumed). The growth media for PDC production is the second largest positive contributor (1.64 kg CO_2e per kg), and there is also significant impact from the hydrolysis block mainly from glucose purchase for onsite enzyme production.

Furthermore, grid carbon intensity varies widely across regions—from ~0.020 to 0.887 kgCO_2e per kWh within the U.S. (2019–2023 averages).[28] Sensitivity analysis (Fig. S4) showed the carbon footprint increases to 1.59 kgCO_2e per kg Na $(PDC)_2$-salt at the lowest grid intensity and decreases to

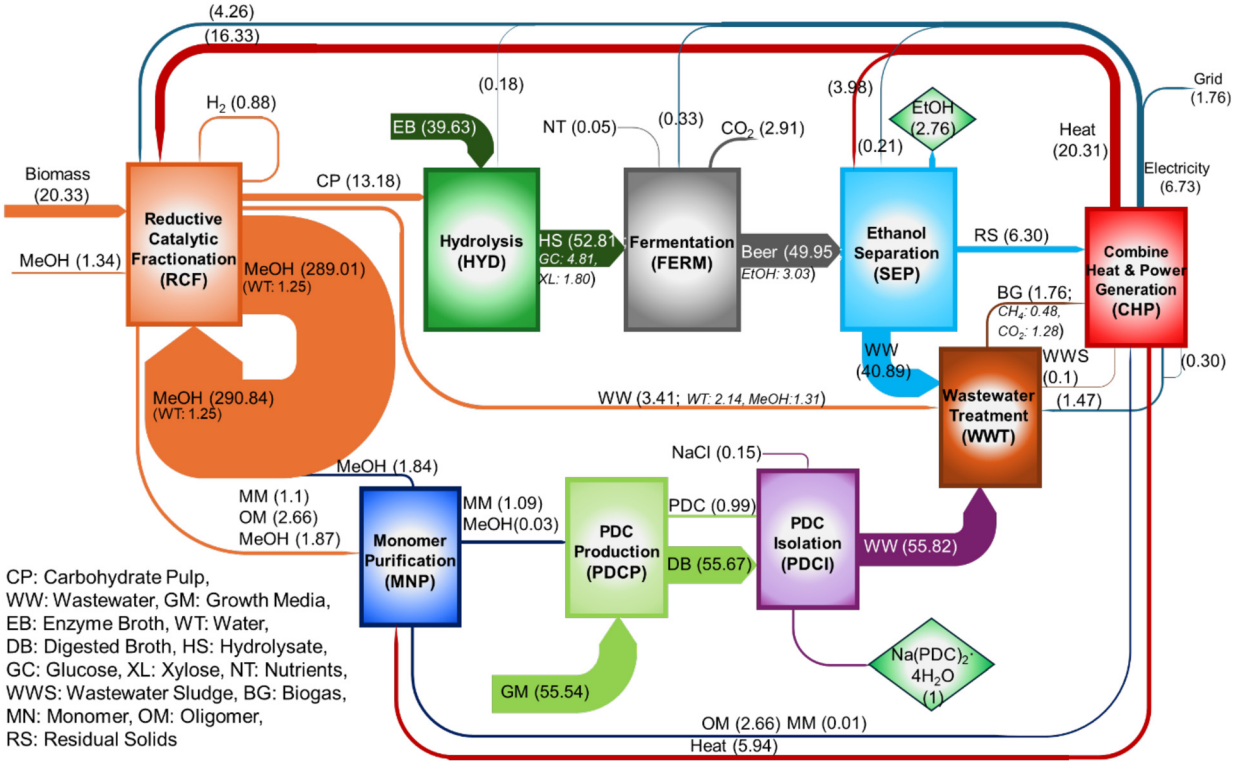

Fig. 4 Normalized mass and energy flow to produce 1 kg of $Na(PDC)_2{\cdot}4H_2O$ salt. Electricity and heat flows are in kWh; all mass flows are in kg.

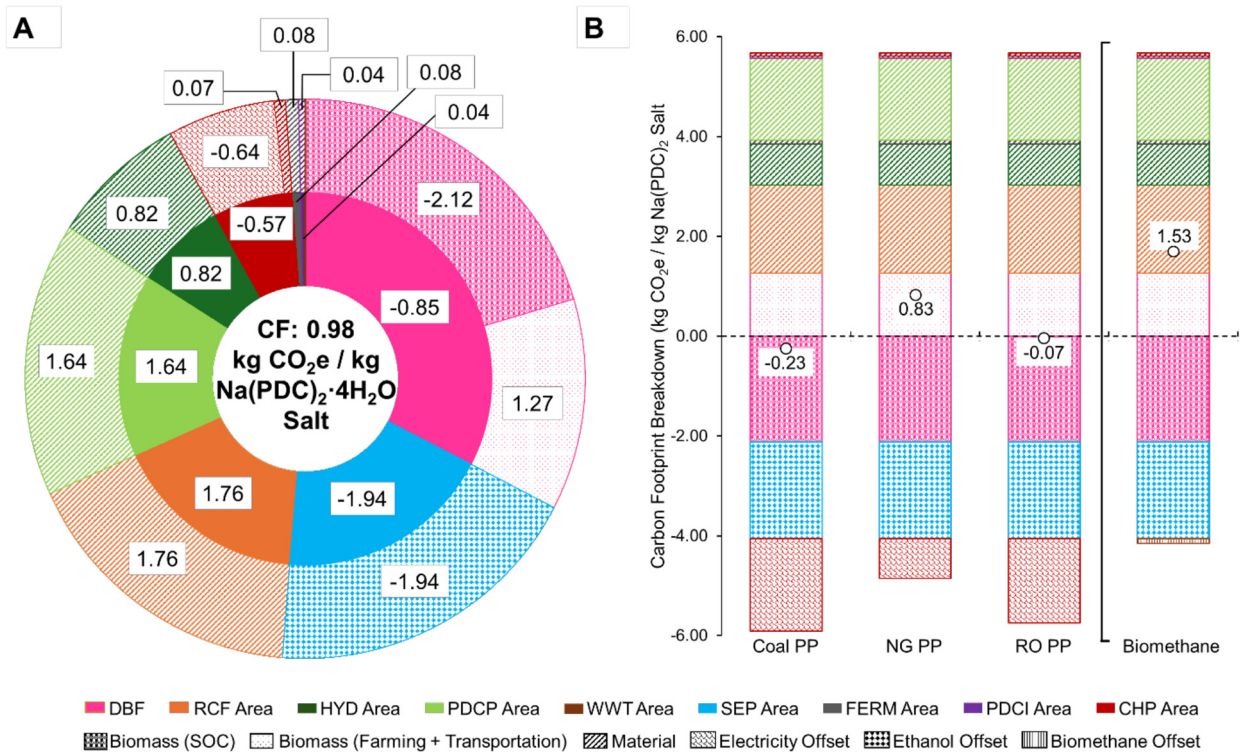

Fig. 5 Breakdown of contribution to the carbon footprint for production of 1 kg of $Na(PDC)_2{\cdot}4H_2O$ salt. (A) Base case (B) extensions: electricity offset from coal, natural gas (NG), and residual oil (RO) power plant (PP). Abbreviations: DBF: Delivered Biomass Feedstock; the other abbreviations mean the same as initially declared.

0.06 kgCO_2e per kg at the highest intensity. This reflects the smaller emission offsets in low-intensity grids and larger offsets in carbon-intensive grids.

As the source of electricity that is offset is crucial, we extended the analysis to examine electricity offset from three different power plants (Fig. 5B), first three stacked plots. Substantial emission offset was achieved resulting in a negative footprint if we offset electricity from coal and residual oil power plants (−1.85 and −1.69 kg CO_2e per kg of product, respectively). Finally, co-producing biomethane rather than electricity, led to the highest net footprint of 1.53 kg CO_2e per kg of product, due to lower emission offset associated with displacing fossil-based natural gas.

Conclusions

This work advances previous efforts that demonstrated microbial funneling of depolymerized lignin to a value-added product, using engineered *N. aromaticivorans*. In that approach, isolated lignin was depolymerized before biological upgrading, resulting in a cost-intensive commodity chemical production pipeline. In contrast, the current study presents a fully integrated, lignin-first design in which biomass fractionation and lignin depolymerization occur in a single RCF step. We found that this tandem process provided both improved phenolic monomer yields for conversion to a product, while generating high-quality cellulose-pulp for fermentation into ethanol. In addition to the economic analysis, we assess the positive carbon footprint of this integrated process.

The results indicate that the MSP of $Na(PDC)_2$ salt is $18.39 per kg, with a corresponding net carbon footprint of 0.98 kgCO_2e per kg. The proposed tandem process leads to a $7.50 per kg (~29%) reduction in cost due to improved monomer yields and lower biomass cost. Our analysis shows that the RCF block has the highest cost contribution due to a high solvent-to-biomass ratio affecting equipment capital costs. Reducing the solvent-to-biomass ratio from 17.25 : 1 to 12 : 1 achieves the highest reduction in MSP (~24%) while co-producing biomethane rather than electricity reduces the MSP by ~4%. From a sustainability standpoint, the solvent make-up and growth media needed for enzymatic funneling to PDC are the major contributors to carbon footprint. We further observe that soil organic carbon sequestration associated with biomass (poplar) cultivation, and electricity and ethanol offsets provide significant emission reductions. Importantly, the work reported herein describes an integrated and experimentally validated pipeline from raw biomass to multiple products – biofuel, biochemical, and electricity – while achieving improved economic and environmental outcomes.

Experimental

Materials and methods

Commercially available chemicals were purchased from Millipore Sigma (St Louis, MO), Fisher Scientific (Chicago, IL), VWR (Batavia, IL), TCI America (Portland, OR), Acros International (Livingston, NJ), Neta scientific (Hainesport, NJ), and Ambeed (Arlington Heights, IL). Specialty gases (*i.e.*, hydrogen, argon, and helium) were purchased from Airgas (Madison, WI). The palladium on carbon (Pd/C) catalyst used in this study was 5 wt% palladium on a matrix of activated carbon support (Millipore Sigma P/N: 205680). The catalyst was used as received.

Poplar biomass preparation

The NM6 hybrid poplar (*Populus maximowiczii* × *nigra*) was produced by the Great Lakes Bioenergy Research Center and used in previous studies.[12,29] The NM6 trees were nearly 5-year-old (59 month) at harvest, the bark was removed, and the xylem tissue was chipped, sorted on a shaker table to pass through 5 mm round hole, and then air dried. After drying the particle size was further homogenized, by grinding the poplar chips into a flour using a shaker mill (Retch MM400, 50 mL hardened steel jar, 1 × 15 mm hardened steel grinding ball, 30 Hz for 3 min). The powdered biomass was used without any further processing. Characterization of the biomass composition can be found in the SI of Perez *et al.* 2022 and Pastore de Lima *et al.* 2024.[12,29]

Hydrogenolysis of poplar biomass

Hydrogenolysis of poplar biomass was performed in a 50 mL Parr reactor. Briefly, 1.377 g of poplar flour was placed into the reactor. To this was added 76 mg of Pd/C as the active catalyst, which was used without any pretreatment. Then 30 mL methanol and 65 nmol 1,2-dimethoxybenzene (DMB, internal standard) were added into the reactor. The reactor was then sealed, and the reaction mixture was purged with Argon three times, followed by purging three times with hydrogen, before finally being pressurized to 30 bars with hydrogen. The vessel was placed in the furnace and the reactor was heated up to 200 °C and the pressure increased to 65 bar. After 2 h of reaction, the reactor was cooled to room temperature with air flow. The product mixture was filtered through a 2 μm filter and the hydrogenolysis oil was stored at 4 °C. The phenolic monomer composition was quantified on a Shimadzu GC-2010Plus with an FID detector, Table 2, as was previously described.[12] The treated biomass solid residue, which consisted of the polysaccharides (cellulose and hemicellulose), residual lignin, and the Pd/C catalyst, was dried under vacuum (<15 mTorr) for 16 h. The dried residue was stored at room temperature and used in the enzymatic digestion and fermentation study without further treatment.

Bacterial strains and culture conditions

The engineered strain of *N. aromaticivorans* DSM12444 lacking the genes Saro_1879 (*sacB*), Saro_2819 (*ligI*), and Saro_2864/5 (*desC*/*desD*),[30] was used in this study. Cultures were grown in SMB media supplemented with the indicated carbon source at 30 °C. SMB media contains 20 mM Na_2HPO_4, 20 mM KH_2PO_4, 7.5 mM $(NH_4)_2SO_4$, 0.167 mM $ZnSO_4$, 0.125 mM $FeSO_4$, 0.028 mM $MnSO_4$, 0.006 mM $CuSO_4$, 0.009 mM $Co(NO_3)_2$,

0.016 mM $Na_2B_4O_7$, 24.319 mM $MgSO_4$, 1.667 mM $CaCl_2$, 0.013 mM $(NH_4)_6Mo_7O_{24}$. For routine culture and storage, the growth media was supplemented with 1 g L^{-1} glucose.

Depolymerized lignin bioconversion experiments

Bioconversion experiments were performed following the protocol described in Perez *et al.* 2022.[12] Briefly, the PDC-producing *N. aromaticivorans* strain PDC cultures was pregrown overnight in 10 mL of SMB medium supplemented with 6 mM glucose. The bioconversion experiments were initiated by diluting the cultures with 10 mL SMB medium supplemented with 12 mM glucose and 20 mL L^{-1} of the RCF oil in MeOH (the RCF solvent). Triplicate culture assays were grown for 25 h in flasks at 30 °C and shaken at 200 rpm. The bacterial cell density was monitored periodically using a Klett-Summerson photoelectric colorimeter with a red filter. Sample aliquots were periodically removed from the cultures, filtered with a 0.2 μm PES syringe filter, and stored at −20 °C for further analysis of aromatic metabolites, PDC, and glucose as described previously.[12]

Hydrolysate production by enzyme digestion

Hydrolysates were produced from hydrogenolysis-treated biomass solid residue by enzymatic digestion using a two-step enzyme-loading strategy, as previously described.[31] To obtain a 7% glucan loading, 85 mL Oak Ridge centrifuge tubes (Thermo Fisher Scientific Inc., Waltham, MA, USA) were loaded at a solid-to-liquid ratio of 1 : 4, with approximately 7 g hydrogenolysis treated biomass solids, 16.3 mL water, and 3.5 mL 1 M phosphate buffer (126.17 g L^{-1} KH_2PO_4 and 11.32 g L^{-1} K_2HPO_4). The tubes were autoclaved for 1 h at 121 °C. After cooling to 50 °C, 0.15 mL of undiluted HCl (~37–38% HCl, w/w) followed by 5 mL of 1 M phosphate buffer were added to adjust a pH of 5.8. Enzymatic digestion was initiated by adding 4.1 mL of an enzyme mixture containing 0.7 mL cellulase (NS 22257, Novozymes, Franklinton, NC, USA) and 0.12 mL xylanase (NS 22244, Novozymes, Franklinton, NC, USA) diluted in 3.3 mL of MilliQ water. The digesting suspension was placed on a BT LabSystems vertical rotating mixer (St Louis, MO, USA). The rotating mixer was inside a Bellco Biotechnology bench top incubator (VineLand NJ, USA) that was set to 50 °C and 70 rpm stirring. After 48 h, a second 4.1 mL dose of the enzyme mixture was added, and digestion was continued for an additional 6 days at 50 °C and 70 rpm. After 7 days of digesting, the final pH of the sample was ~5.2. The solids were removed by centrifugation at 8200*g* at 4 °C for 2 h followed by decanting the supernatant (hydrolysate). The pH of the hydrolysate was adjusted to 5.8 using 10 M NaOH or undiluted HCl, filtered-sterilized through a 0.2 μm aPES Nalgene Rapid-Flow 50 mm bottle top filter, and stored at 4 °C until it was use in fermentation experiments. HPLC-RID analysis of the concentration of glucose, xylose, cellulobiose was performed on an Agilent series 1200 HPLC (Santa Clara, CA, USA) equipped with 0.01 N H_2SO_4 mobile phase at 0.5 mL min^{-1} and an Aminex 87H column (BioRad, Hercules, CA, USA) as described previously.[31]

Fermentation of the hydrolysate

The approach used to ferment hydrolysates into ethanol by yeast have been previously described.[31] *S. cerevisiae* GLBRCY945[32] was prepared from frozen glycerol stocks by isolating colonies onto yeast-peptone-dextrose (YPD; 20 g L^{-1} peptone, 20 g L^{-1} glucose, 10 g L^{-1} yeast extract) agar grown overnight under aerobic conditions at 30 °C and sub-cultured into YPD broth under similar conditions with shaking at 225 rpm. After 12 h, the cultures were centrifuged, and the cell pellets were resuspended in MilliQ water and inoculated into sterile Wheaton Serum Bottles (60 mL) containing 4 mL of the hydrogenolysis treated poplar hydrolysate to achieve a starting OD600 of 0.5. Serum bottles were capped under aseptic conditions with a sterile butyl rubber cap, punctured with a sterile needle connected to a gas manifold and vacuum pump to remove air and flush with nitrogen gas. Serum bottles were connected to a respirometer (AER-800; Challenge Technology; Springdale, AR, USA) using sterile needles (23 gauge) and placed in an orbital shaker (Innova 2300, New Brunswick, Edison NJ, USA) at 180 rpm. The volume of gas or carbon dioxide (CO_2) produced by the culture was measured in real-time over the 60 h fermentation. Final cell density (OD600) measurements were made with a spectrophotometer (UV-1280, Shimadzu Scientific Instruments, Columbia MD, USA). Supernatants of fermentation broth at the end of fermentation were analyzed by HPLC-RID analysis for glucose, xylose, cellobiose, ethanol, and other end-products as described previously.[31] Process ethanol yields, expressed as the percentage of maximal theoretical ethanol yield (0.51 g ethanol per g sugar) produced from the total glucose and xylose present in each hydrolysate, were calculated from the initial sugar and final sugar and ethanol concentrations for each experiment.

Techno-economic analysis

The key data used in the analysis for the biorefinery are reported in Table 3. The economic analysis in this study is performed using the net present value (NPV) approach to calculate the MSP of $Na(PDC)_2$ salt required to support the sale of

Table 3 Key plant design data

Basis	Description	
Capacity	2000 metric ton per day of dry biomass	
Block	Process condition	
RCF	Reaction condition	200 °C, 65 bar, 2 h
	Dry biomass : methanol : hydrogen	1 : 17.25 : 0.052[a]
	Dry biomass : catalyst (5 wt% Pd/C)	1 : 0.056[a]
	Catalyst lifetime	1 year
	Dry biomass-to-monomer yield	6.5%
	Carbohydrate retention	70%
PDCP	Reaction condition	30 °C, 1 atm, 25 h
	Monomer-to-PDC yield	90%
HYD	Glucose concentration in hydrolysate	112 g L^{-1}
	Xylose concentration in hydrolysate	42 g L^{-1}
FERM	Glucose conversion to ethanol	100%
	Xylose conversion to ethanol	62%

[a] Mass ratio.

ethanol product at $2.50 per gasoline gallon equivalent. We first compute the total capital investment (TCI) based on the total equipment cost. The TCI entails the total direct cost, total indirect cost, and working capital. Next, we determine the annual fixed and variable operating costs. The fixed operating cost entails labor, supervision, and other overhead costs, while the variable operating cost includes biomass feedstock, makeup methanol and hydrogen, catalyst, and other process related raw material costs. Finally, we determine the MSP based on a developed optimization model. The economic data and assumptions, Table S5.[9,14,24–27,33–39]

Life cycle analysis

We perform carbon footprint analysis using the material and energy balance from the process model used for calculating the MSP with emission factors sourced from Argonne GREET® model[40] and the literature,[41] Table S6. The functional unit for the life cycle analysis (LCA) is 1 kg of $Na(PDC)_2$ salt. The system boundary entails biomass (poplar) farming and transportation to the biorefinery, and material and energy inputs at the biorefinery. We consider offset emissions associated with surplus electricity by assuming the electricity displaces U.S. grid electricity. We further consider emission offsets with ethanol by assuming ethanol displaces emissions from fossil-based gasoline. We assume biogenic CO_2 emissions are carbon neutral. We then calculate the carbon footprint of the $Na(PDC)_2$ salt on a per kg basis. The analysis is extended by examining various cases where the electricity sold offset emissions from electricity generated by different power plants: coal, residual oil, and natural gas. We also present an analysis for the case in which biomethane is co-produced rather than electricity.

Author contributions

Project lead and administration: CS; project conceptualization: CS, SK, CM, DN; performed the investigation: CS, EA, SK, JP, GU, YZ, JS; funding acquisitions: TD, CS, SK, DN, CM; visualization: CS, EA, SK; writing – original draft: CS, EA, SK, YZ, JS; writing – review & editing: CS, EA, SK, JP, TD, DN, CM.

Conflicts of interest

There are no conflicts to declare.

Data availability

The data supporting this article have been included as part of the supplementary information (SI). Supplementary information is available. See DOI: https://doi.org/10.1039/d5gc03986j.

Acknowledgements

This material is based upon work supported by the Great Lakes Bioenergy Research Center, U.S. Department of Energy, Office of Science, Office of Biological and Environmental Research under Award Number DE-SC0018409. The authors thank Kyle Prost for his help in editing the experimental description for hydrolysate production and fermentation to ethanol.

References

1 M. M. Abu-Omar, K. Barta, G. T. Beckham, J. S. Luterbacher, J. Ralph, R. Rinaldi, Y. Román-Leshkov, J. S. M. Samec, B. F. Sels and F. Wang, Guidelines for performing lignin-first biorefining, *Energy Environ. Sci.*, 2021, **14**(1), 262–292.

2 T. I. Korányi, B. Fridrich, A. Pineda and K. Barta, Development of 'lignin-first' approaches for the valorization of lignocellulosic biomass, *Molecules*, 2020, **25**(12), 2815.

3 L. Shuai, M. T. Amiri, Y. M. Questell-Santiago, F. Héroguel, Y. Li, H. Kim, R. Meilan, C. Chapple, J. Ralph and J. S. Luterbacher, Formaldehyde stabilization facilitates lignin monomer production during biomass depolymerization, *Science*, 2016, **354**(6310), 329–333.

4 J. S. Luterbacher, A. Azarpira, A. H. Motagamwala, F. Lu, J. Ralph and J. A. Dumesic, Lignin monomer production integrated into the γ-valerolactone sugar platform, *Energy Environ. Sci.*, 2015, **8**(9), 2657–2663.

5 B. Daelemans, B. Sridharan, P. Jusner, A. Mukherjee, J. Chen, J. K. Kenny, M. Van Dael, K. Vanbroekhoven, P. J. Deuss, M. L. Stone and E. Feghali, From lignin to market: a technical and economic perspective of reductive depolymerization approaches, *Green Chem.*, 2025, DOI: 10.1039/D5GC02316E.

6 F. Brienza, D. Cannella, D. Montesdeoca, I. Cybulska and D. P. Debecker, A guide to lignin valorization in biorefineries: traditional, recent, and forthcoming approaches to convert raw lignocellulose into valuable materials and chemicals, *RSC Sustainability*, 2024, **2**(1), 37–90.

7 X. Wu, E. Smet, F. Brandi, D. Raikwar, Z. Zhang, B. U. W. Maes and B. F. Sels, Advancements and perspectives toward lignin valorization via O-demethylation, *Angew. Chem., Int. Ed.*, 2024, **63**(10), e202317257.

8 W. Schutyser, T. Renders, S. Van den Bosch, S.-F. Koelewijn, G. T. Beckham and B. F. Sels, Chemicals from lignin: an interplay of lignocellulose fractionation, depolymerisation, and upgrading, *Chem. Soc. Rev.*, 2018, **47**(3), 852–908.

9 D. M. Alonso, S. H. Hakim, S. Zhou, W. Won, O. Hosseinaei, J. Tao, V. Garcia-Negron, A. H. Motagamwala, M. A. Mellmer, K. Huang, C. J. Houtman, N. Labbe, D. P. Harper, C. Maravelias, T. Runge and J. A. Dumesic, Increasing the revenue from

lignocellulosic biomass: Maximizing feedstock utilization, in *Science Advances*, 2017/06/01 ed, 2017, vol. 3, pp. 1–7.

10 T. Renders, G. Van den Bossche, T. Vangeel, K. Van Aelst and B. Sels, Reductive catalytic fractionation: State of the art of the lignin-first biorefinery, *Curr. Opin. Biotechnol.*, 2019, **56**, 193–201.

11 E. M. Anderson, M. L. Stone, R. Katahira, M. Reed, G. T. Beckham and Y. Román-Leshkov, Flowthrough reductive catalytic fractionation of biomass, *Joule*, 2017, **1**(3), 613–622.

12 J. M. Perez, C. Sener, S. Misra, G. E. Umana, J. Coplien, D. Haak, Y. Li, C. T. Maravelias, S. D. Karlen, J. Ralph, T. J. Donohue and D. R. Noguera, Integrating lignin depolymerization with microbial funneling processes using agronomically relevant feedstocks, *Green Chem.*, 2022, **24**(7), 2795–2811.

13 F. Cheng, S. Liu, S. D. Karlen, H. Kim, F. Lu, J. Ralph, L. M. Vázquez Ramos, G. Huber and J. A. Dumesic, Poplar Lignin structural changes during extraction in γ-valerolactone (GVL), *Green Chem.*, 2023, **25**(1), 336–347.

14 A. W. Bartling, M. L. Stone, R. J. Hanes, A. Bhatt, Y. Zhang, M. J. Biddy, R. Davis, J. S. Kruger, N. E. Thornburg, J. S. Luterbacher, R. Rinaldi, J. S. M. Samec, B. F. Sels, Y. Roman-Leshkov and G. T. Beckham, Techno-economic analysis and life cycle assessment of a biorefinery utilizing reductive catalytic fractionation, *Energy Environ. Sci.*, 2021, **14**(8), 4147–4168.

15 Y. Mottiar, S. D. Karlen, R. E. Goacher, J. Ralph and S. D. Mansfield, Metabolic engineering of *p*-hydroxybenzoate in poplar lignin, *Plant Biotechnol. J.*, 2023, **21**(1), 176–188.

16 J. S. Luterbacher, J. M. Rand, D. M. Alonso, J. Han, J. T. Youngquist, C. T. Maravelias, B. F. Pfleger and J. A. Dumesic, Nonenzymatic sugar production from biomass using biomass-derived γ-valerolactone, *Science*, 2014, **343**(6168), 277–280.

17 Z. Sun, B. Fridrich, A. de Santi, S. Elangovan and K. Barta, Bright side of lignin depolymerization: Toward new platform chemicals, *Chem. Rev.*, 2018, **118**(2), 614–678.

18 K. M. Torr, D. J. van de Pas, E. Cazeils and I. D. Suckling, Mild hydrogenolysis of *in situ* and isolated *Pinus radiata* lignins, *Bioresour. Technol.*, 2011, **102**(16), 7608–7611.

19 C. Sener, V. I. Timokhin, J. Hellinger, J. Ralph and S. D. Karlen, Pd/C promotes C–H bond activation and oxidation of *p*-hydroxybenzoate during reductive catalytic fractionation of poplar, *Nat. Commun.*, 2025, **16**, 5259.

20 B. Kim, J. M. Perez, S. D. Karlen, J. Coplien, T. J. Donohue and D. R. Noguera, Achieving high productivity of 2-pyrone-4,6-dicarboxylic acid from aqueous aromatic streams with *Novosphingobium aromaticivorans*, *Green Chem.*, 2024, **26**, 7997–8009.

21 M. Perez, W. Kontur, M. Alherech, S. D. Karlen, S. Stahl, T. J. Donohue and D. R. Noguera, Funneling aromatic products of chemically depolymerized lignin into 2-pyrone-4–6-dicarboxylic acid with *Novosphingobium aromaticivorans*, *Green Chem.*, 2019, **21**(6), 1340–1350.

22 S. Zhou, M. García Mancilla, J. Francis Clar, T. M. Runge, T. J. Donohue, D. R. Noguera and S. D. Karlen, Biotransformation of Phenolics in Spent Liquor from Aqueous Ammonia Pretreatment, *ChemSusChem*, 2025, **Sep 10**, e2500881.

23 F. Metz, A. M. Olsen, F. Lu, K. S. Myers, M. N. Allemann, J. K. Michener, D. R. Noguera and T. J. Donohue, Catabolism of β-5 linked aromatics by Novosphingobium aromaticivorans, *Appl. Ind. Microbiol.*, 2024, **15**(8), e01718–e01724.

24 D. Humbird, R. Davis, L. Tao, C. Kinchin, D. Hsu, A. Aden, P. Schoen, J. Lukas, B. Olthof, M. Worley, D. Sexton and D. Dudgeon, *Process design and economics for biochemical conversion of lignocellulosic biomass to ethanol: Dilute-acid pretreatment and enzymatic hydrolysis of corn stover; NREL/TP-5100-47764*, *National Renewable Energy Lab, Golden, CO (United States*, 2011, **303**.

25 Crux, *Renewable natural gas for tax credit buyers*, 2024. https://www.cruxclimate.com/insights/rng-for-tax-credit-buyers, (accessed on December 12, 2024).

26 United States Environmental Protection Agency (US EPA), *RIN trades and price information*, 2024. https://www.epa.gov/fuels-registration-reporting-and-compliance-help/rin-trades-and-price-information, (accessed on December 21, 2024).

27 United States, Department of Energy, Alternative Fuels Data Center, *Clean fuel production credit*, 2024, https://afdc.energy.gov/laws/13321, (accessed on December 21, 2024).

28 United States Environmental Protection Agency (US EPA), *Historical eGRID Data*, 2024, https://www.epa.gov/egrid/historical-egrid-data, (accessed on November 29, 2024).

29 A. E. Pastore de Lima, J. Coplien, L. C. Anthony, T. Sato, Y. Zhang, S. D. Karlen, C. T. Hittinger and C. T. Maravelias, On the synthesis of biorefineries for high-yield isobutanol production: from biomass-to-alcohol experiments to system level analysis, *RSC Sustainability*, 2024, **2**, 2532–2540.

30 J. M. Perez, W. S. Kontur, M. Alherech, J. Coplien, S. D. Karlen, S. S. Stahl, T. J. Donohue and D. R. Noguera, Funneling aromatic products of chemically depolymerized lignin into 2-pyrone-4-6-dicarboxylic acid with Novosphingobium aromaticivorans, *Green Chem.*, 2019, **21**(6), 1340–1350.

31 J. Serate, D. Xie, E. Pohlmann, C. Donald, M. Shabani, L. Hinchman, A. Higbee, M. Mcgee, A. La Reau, G. E. Klinger, S. Li, C. L. Myers, C. Boone, D. M. Bates, D. Cavalier, D. Eilert, L. G. Oates, G. Sanford, T. K. Sato, B. Dale, R. Landick, J. Piotrowski, R. G. Ong and Y. P. Zhang, Controlling microbial contamination during hydrolysis of AFEX-pretreated corn stover and switchgrass: effects on hydrolysate composition, microbial response and fermentation, *Biotechnol. Biofuels*, 2015, **8**(180), 1–17.

32 L. S. Parreiras, R. J. Breuer, R. Avanasi Narasimhan, A. J. Higbee, A. La Reau, M. Tremaine, L. Qin, L. B. Willis, B. D. Bice, B. L. Bonfert, R. C. Pinhancos, A. J. Balloon, N. Uppugundla, T. Liu, C. Li, D. Tanjore, I. M. Ong, H. Li, E. L. Pohlmann, J. Serate, S. T. Withers, B. A. Simmons, D. B. Hodge, M. S. Westphall, J. J. Coon, B. E. Dale, V. Balan, D. H. Keating, Y. Zhang, R. Landick, A. P. Gasch and T. K. Sato, Engineering and two-stage evolution of a

lignocellulosic hydrolysate-tolerant *Saccharomyces cerevisiae* strain for anaerobic fermentation of xylose from AFEX pretreated corn stover, *PLoS One*, 2014, **9**(9), e107499.

33 R. E. Davis, N. J. Grundl, L. Tao, M. J. Biddy, E. C. Tan, G. T. Beckham, D. Humbird, D. N. Thompson and M. S. Roni, *Process design and economics for the conversion of lignocellulosic biomass to hydrocarbon fuels and coproducts: 2018 Biochemical design case update; Biochemical deconstruction and conversion of biomass to fuels and products via integrated biorefinery pathways; NREL/TP-5100-71949*, National Renewable Energy Laboratory (NREL), Golden, CO, USA, 2018.

34 R. Davis, L. Tao, C. Scarlata, E. C. D. Tan, J. Ross, J. Lukas and D. Sexton, *Technical report: Process design and economics for the conversion of lignocellulosic biomass to hydrocarbons: dilute-acid and enzymatic deconstruction of biomass to sugars and catalytic conversion of sugars to hydrocarbons; NREL/TP-5100-62498*, National Renewable Energy Lab. (NREL), Golden, CO, USA, 2015.

35 Chemical market price for Pd/C catalyst, Alibaba Group, 2024, https://www.alibaba.com/trade/search?spm=a2700.galleryofferlist.the-new-header_fy23_pc_search_bar.searchButton&tab=all&SearchText=5+wt%25+Pd%2FC+catalyst, (accessed on October 19, 2024).

36 United States Energy Information Administration (US EIA), *Electric Power Monthly*, 2024, https://www.eia.gov/electricity/monthly/epm_table_grapher.php, (accessed on December 21, 2024).

37 Ammonium sulfate prices Worldwide | Historical and current | Intratec, 2025, https://www.intratec.us/chemical-markets/ammonium-sulfate-price, (accessed on December 21, 2024).

38 Y. Liao, S. F. Koelewijn, G. Van den Bossche, J. Van Aelst, S. Van den Bosch, T. Renders, K. Navare, T. Nicolai, K. Van Aelst, M. Maesen, H. Matsushima, J. M. Thevelein, K. Van Acker, B. Lagrain, D. Verboekend and B. F. Sels, A sustainable wood biorefinery for low-carbon footprint chemicals production, *Science*, 2020, **367**(6484), 1385–1390.

39 A. J. Karres, *What is industrial salt supply and how much does it cost?* Advantage water conditioning, 2020, https://www.indywaterpros.com/blog/industrial-salt-supply-cost, (accessed on December 21, 2024).

40 M. Wang, A. Elgowainy, U. Lee, K. H. Baek, S. Balchandani, P. T. Benavides, A. Burnham, H. Cai, P. Chen, Y. Gan, U. R. Gracida-Alvarez, T. R. Hawkins, T.-Y. Huang, R. K. Iyer, S. Kar, J. C. Kelly, T. Kim, C. P. Kolodziej, K. Lee, X. Liu, Z. Lu, F. H. Masum, M. Morales, C. Ng, L. Ou, T. K. Poddar, K. Reddi, S. Shukla, U. Singh, L. Sun, P. Sun, P. Vyawahare and J. Zhang, *Summary of Expansions and Updates in R&D*, GREET®, 2023, ANL/ESIA-23/10, Argonne National Laboratory (ANL), Lemont, IL USA, p. 2023.

41 I. Gelfand, S. K. Hamilton, A. N. Kravchenko, R. D. Jackson, K. D. Thelen and G. P. Robertson, Empirical Evidence for the Potential Climate Benefits of Decarbonizing Light Vehicle Transport in the U.S. with Bioenergy from Purpose-Grown Biomass with and without BECCS, *Environ. Sci. Technol.*, 2020, **54**(5), 2961–2974.